Biochimica et Biophysica Acta 1831 (2013) 769–775

Contents lists available at SciVerse ScienceDirect

Biochimica et Biophysica Acta

journal homepage: www.elsevier.com/locate/bbalip

# Cholesterol reduction ameliorates glucose-induced calcium handling and insulin secretion in islets from low-density lipoprotein receptor knockout mice

J.C. Souza [a], E.C Vanzela [a], R.A. Ribeiro [a,1], L.F. Rezende [a], C.A. de Oliveira [a,b], E.M. Carneiro [a], H.C.F. Oliveira [a], A.C. Boschero [a,*]

[a] Department of Structural and Functional Biology, Institute of Biology, State University of Campinas (UNICAMP), Campinas, SP, Brazil
[b] Department of Biosciences, Federal University of Sao Paulo (Unifesp), Santos, SP, Brazil

ARTICLE INFO

*Article history:*
Received 31 July 2012
Received in revised form 10 December 2012
Accepted 27 December 2012
Available online 6 January 2013

*Keywords:*
Calcium handling
Cholesterol
Glucose
Insulin secretion
LDLR$^{-/-}$ mice
SNARE proteins

ABSTRACT

*Aims/hypothesis:* Changes in cellular cholesterol level may contribute to beta cell dysfunction. Islets from low density lipoprotein receptor knockout (LDLR$^{-/-}$) mice have higher cholesterol content and secrete less insulin than wild-type (WT) mice. Here, we investigated the association between cholesterol content, insulin secretion and $Ca^{2+}$ handling in these islets.
*Methods:* Isolated islets from both LDLR$^{-/-}$ and WT mice were used for measurements of insulin secretion (radioimmunoassay), cholesterol content (fluorimetric assay), cytosolic $Ca^{2+}$ level (fura-2AM) and SNARE protein expression (VAMP-2, SNAP-25 and syntaxin-1A). Cholesterol was depleted by incubating the islets with increasing concentrations (0–10 mmol/l) of methyl-beta-cyclodextrin (MβCD).
*Results:* The first and second phases of glucose-stimulated insulin secretion (GSIS) were lower in LDLR$^{-/-}$ than in WT islets, paralleled by an impairment of $Ca^{2+}$ handling in the former. SNAP-25 and VAMP-2, but not syntaxin-1A, were reduced in LDLR$^{-/-}$ compared with WT islets. Removal of excess cholesterol from LDLR$^{-/-}$ islets normalized glucose- and tolbutamide-induced insulin release. Glucose-stimulated $Ca^{2+}$ handling was also normalized in cholesterol-depleted LDLR$^{-/-}$ islets. Cholesterol removal from WT islets by 0.1 and 1.0 mmol/l MβCD impaired both GSIS and $Ca^{2+}$ handling. In addition, at 10 mmol/l MβCD WT islet showed a loss of membrane integrity and higher DNA fragmentation.
*Conclusion:* Abnormally high (LDLR$^{-/-}$ islets) or low cholesterol content (WT islets treated with MβCD) alters both GSIS and $Ca^{2+}$ handling. Normalization of cholesterol improves $Ca^{2+}$ handling and insulin secretion in LDLR$^{-/-}$ islets.

© 2013 Elsevier B.V. All rights reserved.

## 1. Introduction

Type 2 diabetes is a complex disease characterized by reduced insulin secretion and development of insulin resistance [1]. Frequently, diabetic patients exhibit dyslipidemia with low levels of high-density lipoprotein [2], hypertriglyceridemia [3,4] and increased and abnormal (glycated and/or oxidized) small, dense LDL particles [5]. Chronic influx of fatty acids into beta cells impairs insulin secretion [6,7]; however, emerging evidence also suggests that changes in cellular cholesterol level may contribute to beta cell dysfunction [8–12].

Cholesterol constitutes about 20% of the total membrane lipids and is involved in several subcellular membrane properties, such as thickness and fluidity [13,14]. Disturbance in cholesterol metabolism results in changes in the membrane lipid raft microdomains. Numerous membrane proteins are associated with lipid rafts, including the ion channels Cav1.2 and Kv2.1 [15,16]. Additionally, SNARE proteins (syntaxin-1A, SNAP-25, and VAMP-2) that play an essential role in the fusion of insulin-containing granules to the plasma membrane are linked to these raft microdomains in pancreatic beta cells [17,18].

High beta cell cholesterol levels reduce the effectiveness of the insulin secretory apparatus and also interfere with glucose metabolism by inhibiting glucokinase activity [8,19]. In the absence of a high-fat diet, islets from hypercholesterolemic LDLR$^{-/-}$ mice show higher cholesterol content and reduced insulin secretion in response to glucose [11]. This is associated with decreased glucose uptake and oxidation and lower expression of protein kinase A alpha [11,20]. In this study, we investigated the involvement of $Ca^{2+}$ handling and SNARE protein expression in the reduced insulin response of LDLR$^{-/-}$ mouse islets. We

*Abbreviations:* KRBB, Krebs-Ringer bicarbonate buffer; MβCD, methyl-β-cyclodextrin; RIA, radioimmunoassay

* Corresponding author at: Dept. of Structural and Functional Biology, Institute of Biology, State University of Campinas (Unicamp), Campinas, SP, P.O. Box 6109, Postal code 13083-970 Campinas, SP, Brazil. Tel.: +55 19 3521 6198; fax: +55 19 35216185.
*E-mail address:* boschero@unicamp.br (A.C. Boschero).
[1] Present address: Núcleo em Ecologia e Desenvolvimento Sócio-Ambiental de Macaé (NUPEM), Universidade Federal do Rio de Janeiro (UFRJ), Macaé, RJ, Brazil.

1388-1981/$ – see front matter © 2013 Elsevier B.V. All rights reserved.
http://dx.doi.org/10.1016/j.bbalip.2012.12.013

also investigated the effects of cholesterol depletion on both LDLR$^{-/-}$ and WT islets and their relationships with $Ca^{2+}$ handling and insulin secretion.

## 2. Materials and methods

### 2.1. Animals

LDLR$^{-/-}$ founders were purchased from the Jackson Laboratory (Bar Harbor, ME). Wild-type (WT) mice (C57BL/6 background) were obtained from the breeding colony of the State University of Campinas (UNICAMP). Animal experiments were approved by the University's Committee for Ethics in Animal Experimentation (CEUA/UNICAMP). The mice had free access to standard laboratory rodent chow (Nuvital CR1, Colombo, PR, Brazil) and water and were housed at 22 ± 1 °C on a 12 h light/dark cycle.

### 2.2. Pancreatic islet isolation and static insulin secretion

The pancreatic islets were isolated from fed mice (20 weeks old) by collagenase digestion and then selected with a microscope to exclude any contaminating tissues [21]. After isolation, batches of 4 islets from each group were pre-incubated in Krebs-Ringer bicarbonate buffer (KRBB) containing, in mmol/l: 115 NaCl, 5 KCl, 24 $NaHCO_3$, 2.56 $CaCl_2$, 1 $MgCl_2$ and 25 HEPES, pH 7.4 plus 2.8 mmol/l glucose and 0.3% bovine serum albumin (BSA) for 30 min at 37 °C. The islets were further incubated for 1 h in KRBB containing glucose (2.8 or 11.1 mmol/l) or tolbutamide 100 μmol/l. Aliquots of the supernatant at the end of the incubation period were kept at −20 °C for later insulin measurement by RIA [22].

### 2.3. Perfusion studies

Groups of 50 islets from WT and LDLR$^{-/-}$ mice were placed on a Millipore SW 1300 filter (8 μm pore) in a perfusion chamber (four chambers for each perfusion) and perfused in KRBB buffer for 100 min at a flow rate of 1 ml/min. Glucose (2.8 mmol/l) was present from the onset of the experiment and was elevated to 11.1 mmol/l glucose from the 60th min onward. Solutions were gassed with 95% $O_2$/5% $CO_2$ and maintained at 37 °C. Insulin released into the medium was measured by RIA [22].

### 2.4. Islet cholesterol measurement and depletion

Cholesterol was quantified by a fluorometric method using an enzyme-coupled reaction provided by the Amplex Red Cholesterol Assay kit (Molecular Probes), as previously described [8]. Lipid extraction from groups of 10 islets per mouse performed with chloroform/methanol (2:1 vol/vol), dried under a $N_2$ stream, and diluted in 60 μl of working solution (Amplex Red Cholesterol Assay kit) supplemented with 0.1% Triton X-100. Of this sample, 50 μl was used for the cholesterol assay. For cholesterol depletion, islets were pre-incubated with 0.1, 1 or 10 mmol/l of methyl-β-cyclodextrin (MβCD) (Sigma-Aldrich) at 37 °C for 1 h. Islets were then washed in KRBB (5.6 mmol/l) and used in the experiments.

### 2.5. Cytoplasmic $Ca^{2+}$ oscillations

Fresh pancreatic islets were incubated in KRBB plus 5.6 mmol/l glucose and 5 μmol/l Fura-2/AM for 1 h at 37 °C. Islets previously incubated with MβCD were washed three times with KRBB and incubated with Fura-2/AM, as described above. Islets were then transferred to a thermostatically regulated open chamber (37 °C), placed on the stage of an inverted microscope (Nikon UK, Kingston, UK), and perfused with KRBB at a flow rate of 1.5 ml/min. Islets were then perfused with KRBB that was continuously gassed with 95% $O_2$/5% $CO_2$, pH 7.4 containing 2.8 mmol/l with or without 100 μmol/l tolbutamide or 11.1 mmol/l glucose. A ratio image was acquired at approximately every 5 s with an ORCA-100 CCD camera (Hammamatsu Photonics Iberica, Barcelona, Spain), in conjunction with a Lambda-10-CS dual-filter wheel (Sutter Instrument Company, CA, USA), equipped with 340, 380 nm bandpass filters and a range of neutral-density filters (Omega Opticals, Stanmore, UK). Data were obtained using the ImageMaster3 software (Photon Technology International, NJ, USA). The area under the curve was calculated during the period when the stimulus was present in the medium, after subtracting the basal values (2.8 mmol/l glucose).

### 2.6. Western blotting

Isolated islets from LDLR$^{-/-}$ and WT mice were homogenized in a buffer containing (in mmol/l): 100 Tris pH 7.5, 10 sodium pyrophosphate, 100 sodium fluoride, 10 EDTA, 10 sodium vanadate, and 2 PMSF plus 1% Triton-X 100. The islets were disrupted using a Polytron PT 1200 C homogenizer (Brinkmann Instruments, NY, USA), employing three 10 s pulses. The extracts were then centrifuged at 12,600 *g* at 4 °C for 5 min to remove insoluble material. The protein concentration in the supernatants was assayed using the Bradford dye method [23], using BSA for the standard curve and Bradford reagent (Bio-Agency Lab., São Paulo, SP, BRA). For SDS gel electrophoresis and Western blot analysis, the samples were treated with a Laemmli sample buffer containing dithiothreitol. After heating to 95 °C for 5 min, the proteins were separated by electrophoresis (50 μg protein/lane, 8% gels) and, afterwards, transferred to nitrocellulose membranes. The nitrocellulose membranes were treated overnight with a blocking buffer (5% non-fat dried milk, 10 mmol/l Tris, 150 mmol/l NaCl, and 0.02% Tween 20) and were subsequently incubated with an antibody against SNAP-25 [S-5187; mouse monoclonal; Sigma (St. Louis, MO)], VAMP-2 [627724; rabbit polyclonal; Calbiochem (La Jolla, CA)], or syntaxin-1A [sc-12736; mouse monoclonal; Santa Cruz Biotechnology (Santa Cruz, CA)]. Specific protein bands were visualized by incubating the membranes for 1 h with a peroxidase-conjugated secondary antibody (1:10.000; Zymed Laboratories, Inc., San Francisco, CA, USA), followed by detection with enhanced 151 chemiluminescence reagents (Pierce Biotechnology, USA) and exposure to X-ray film (Kodak, AM, Brazil). The band intensities were quantified by optical densitometry (Un-Scan-It gel, version 6.1, Orem, Utah, USA). After assaying the target proteins, Western blotting was repeated using rabbit polyclonal antibody to GAPDH [1:1.000; cat. (FL-335): sc-25778] as an internal control for protein loading.

### 2.7. Membrane Integrity and DNA fragmentation Assays

Before fragmentation assays, the plasma membranes of a batch of 5 islets were softened with a Tris–HCl buffer containing 0.1% (w/v) SDS at 37 °C for 10 min. After that, the supernatant was collected for DNA quantification, and the islets on the pellet were used for a DNA fragmentation assay using the SYBR Green method, as previously described [24]. DNA leaked from the cytoplasm was expressed of DNA in the supernatant over fragmented DNA [25], considering that membrane integrity is inversely proportional to DNA leakage after membrane softening.

### 2.8. Statistical analysis

The results are presented as means ± SEM for the number of determinations (n) indicated. The data were analyzed by the unpaired Student's *t*-test for two-mean comparisons and one-way ANOVA (with Neumann–Keuls post-hoc test) for dose–response experiments. The level of significance was set at $p<0.05$. Analyses were performed using Statistica version 7.0 for Windows (StatSoft Inc., Tulsa, OK, USA).

## 3. Results

### 3.1. Glucose- and tolbutamide-stimulated insulin release and the $[Ca^{2+}]_i$ rise is reduced in LDLR$^{-/-}$ islets

As previously reported [11], LDLR$^{-/-}$ mice released less insulin in both the first and second phases of GSIS compared with WT mice ($p<0.05$) (Fig. 1). Since the increase in $[Ca^{2+}]_i$ is a key step in insulin secretion, we examined glucose-stimulated $Ca^{2+}$ handling in LDLR$^{-/-}$ islets. A representative example of the $Ca^{2+}$ response to glucose is shown in Fig. 2(A). Elevation of glucose from 2.8 to 11.1 mmol/l induced a $[Ca^{2+}]_i$ rise in both groups; however, the amplitude of oscillations was significantly smaller in LDLR$^{-/-}$ than WT islets. The area under the curve (AUC) of the glucose-evoked $[Ca^{2+}]_i$ rise was significantly reduced in the islets of LDLR$^{-/-}$ mice. A reduction in the AUC of the glucose-evoked $[Ca^{2+}]_i$ in LDLR$^{-/-}$ mice compared to WT was observed in both the first (6 min of exposure to high glucose) and the second phase of insulin release (between min 6 and 20 exposure to high glucose). The AUC of the tolbutamide-evoked $[Ca^{2+}]_i$ rise was also reduced in LDLR$^{-/-}$ islets (Fig. 2.B). Finally, tolbutamide-stimulated insulin secretion was markedly reduced in LDLR$^{-/-}$ islets ($1.22\pm0.16$ vs. $0.50\pm0.11$ ng/islet h, respectively; $p<0.05$).

### 3.2. Reduced expression of SNARE proteins in LDLR$^{-/-}$ islets

Insulin granule exocytosis is a multiple-step process that depends upon the elevation of $[Ca^{2+}]_i$. Since the alterations in $Ca^{2+}$ handling, induced by glucose and tolbutamide, were attenuated in LDLR$^{-/-}$ islets compared with WT islets, it is conceivable that the exocytotic process could also be hampered in the LDLR$^{-/-}$ islets. In fact, the expression of SNAP-25 and VAMP-2, but not syntaxin-1A, was reduced by 30% in LDLR$^{-/-}$ compared with WT islets ($p<0.05$) (Fig. 3).

### 3.3. Reduction in intra-islet cholesterol ameliorates the glucose-stimulated $Ca^{2+}$ rise and insulin secretion in LDLR$^{-/-}$ mice

We have previously shown that cholesterol content is higher in LDLR$^{-/-}$ than in WT islets [11]. Therefore, we analyzed whether the reduction of islet cholesterol content modifies $Ca^{2+}$ handling. For this purpose, islets from both groups were treated with MβCD. Cholesterol content in LDLR$^{-/-}$ islets treated with 0.1 mmol/l MβCD was reduced to levels similar to those found in WT islets (Fig. 4). WT islets treated with 0.1 and 1 mmol/l MβCD showed a marginal decrease in cholesterol content, but at 10 mmol/l MβCD, the cholesterol content was significantly reduced.

Fig. 5(A) shows that MβCD treatment reduced glucose-induced $Ca^{2+}$ oscillations in WT islets. The $[Ca^{2+}]_i$ AUC of MβCD-treated WT islets was lower compared with WT islets without MβCD (Fig. 5C). The tolbutamide-induced $[Ca^{2+}]_i$ rise was significantly reduced in WT islets treated with 10 mmol/l MβCD (Fig. 5D) but was not significantly altered in MβCD-treated LDLR$^{-/-}$ islets (Fig. 5E, F). However, glucose-induced $[Ca^{2+}]_i$ modifications in LDLR$^{-/-}$ islets treated with increasing concentrations of MβCD showed a different behavior compared with WT islets. In these islets, the $[Ca^{2+}]_i$ AUC progressively increased with increasing MβCD concentrations (Fig. 5B). At 0.1 and 1.0 mmol/l MβCD, the $[Ca^{2+}]_i$ rise was similar to that observed in WT islets without MβCD. At 10 mmol/l MβCD, the AUC was significantly higher (2-fold) than in LDLR$^{-/-}$ islets without MβCD (Fig. 5C).

We also examined the relationship between islet cholesterol content and beta cell function. For this purpose, glucose-stimulated insulin secretion was measured in WT and LDLR$^{-/-}$ islets treated with different concentrations of MβCD. Glucose-induced insulin secretion increased with increasing concentrations of MβCD only in LDLR$^{-/-}$ islets (Fig. 6A). In WT islets, there was a significant reduction in glucose-stimulated insulin secretion at 1.0 mmol/l, but a marked increase at 10 mmol/l MβCD. A significant increase in tolbutamide-stimulated insulin release was also observed in WT islets treated with 10 mmol/l MβCD (Fig. 6B). In LDLR$^{-/-}$ islets, tolbutamide-induced insulin secretion at 10 mmol/l MβCD was increased, although to a lesser extent than in WT islets. When LDLR$^{-/-}$ islets were pre-incubated with Simvastatin, an inhibitor of Mevalonato pathway, the calcium handling and insulin secretion were also ameliorated (Figs. 1S and 2S). In WT islets, no significant alterations in the AUC of calcium handling were observed whereas a marginal increment in insulin secretion occurred.

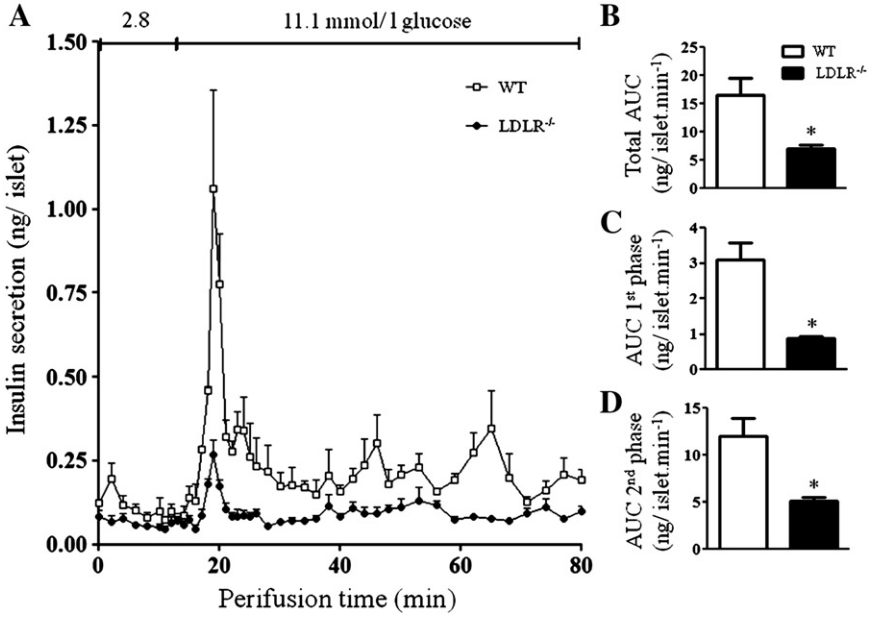


**Fig. 1.** Effects of 11.1 mmol/l glucose on the dynamics of insulin release from WT (open squares and open bars) and LDLR$^{-/-}$ mouse islets (solid circles and dark bars). Groups of 50 freshly isolated islets were perfused for 80 min (A). Glucose at 2.8 mmol/l was present from the onset of the experiment and was increased to 11.1 mmol/l from minute 16 until the end of the perfusion period. (B) Area under the curve of cumulative insulin release measured during the total perfusion time (80 min). (C) AUC of insulin release between time points t = 16 and 22 min (first phase). (D) AUC of insulin release during the second phase, between time points t = 23 and 80 min. Values are means ± SEM of 4 distinct experiments. *$p<0.05$ vs. WT.

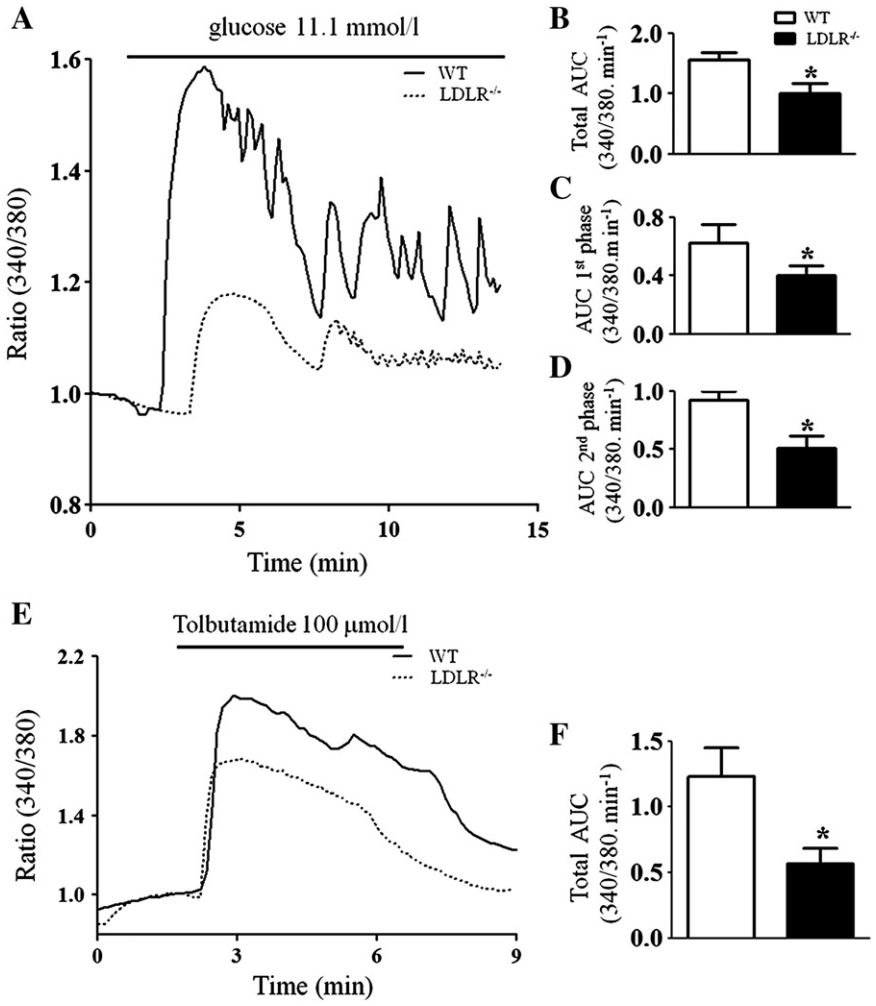


**Fig. 2.** Representative curves of the changes in intracellular $Ca^{2+}$ concentrations in response to 11.1 mmol/l glucose (A) or 100 µmol/l tolbutamide (E) in WT (solid line) and LDLR$^{-/-}$ mouse islets (dotted lines). At 11.1 mmol/l, the area under the curve (AUC) was calculated for 3 different periods: B (1–15 min), C (1–6 min), and D (6–15 min). (F) AUC was calculated when tolbutamide was present in the perfusion period. Values are the ratios of F340/F380 for each group. Data are means ± SEM of 4–7 independent experiments. *p<0.05 indicates significant difference vs. WT.

### *3.4. Intra-islet cholesterol content alters the membrane integrity and DNA fragmentation*

Higher doses of MβCD promote alterations in membrane integrity and DNA fragmentation in WT and LDLR$^{-/-}$ islets. In WT islets, 10 mmol/l MβCD leads to the loss of membrane integrity, provoking a non-specific leakage of cytoplasmic content (Fig. 7A) and an increase DNA fragmentation (Fig. 7B). In LDLR$^{-/-}$ mice the removal of excessive cholesterol content by MβCD reduced DNA fragmentation (Fig. 7B).

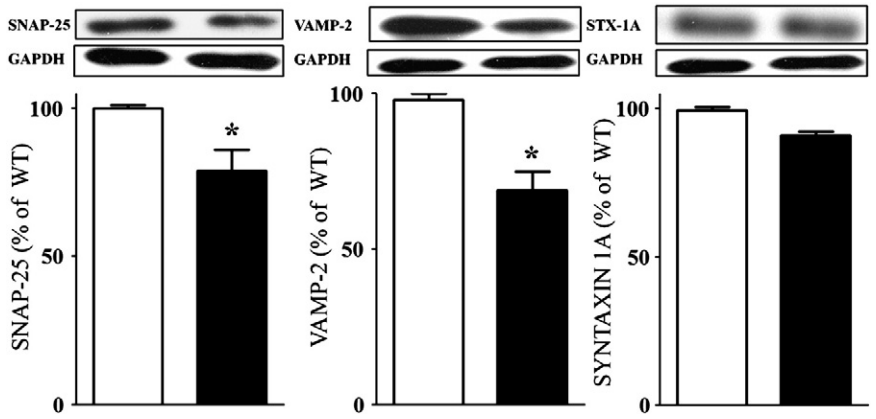


**Fig. 3.** SNAP-25 (A), VAMP-2 (B) and syntaxin-1A protein expression (C) in isolated islets from WT (open bars) and LDLR$^{-/-}$ mice (dark bars). Protein extracts were processed for Western blotting. The bars represent the means ± SEM of the values determined by optical densitometry. n = 3–5; *p<0.05 vs. WT.

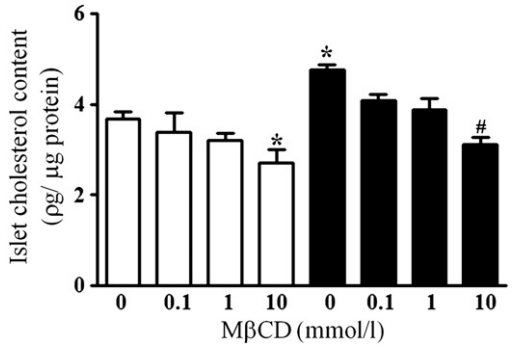


**Fig. 4.** Cholesterol concentrations in islets from WT (open bars) and LDLR$^{-/-}$ mice (dark bars). Cholesterol was depleted in islets using 0.1 mmol/l, 1 mmol/l or 10 mmol/l MβCD for 1 h at 37 °C. Values represent means ± SEM, n = 8–11 mice. $^{*}p<0.05$ vs. WT $^{\#}p<0.05$ vs. LDLR$^{-/-}$ (without MβCD).

## 4. Discussion

Cholesterol content in LDLR$^{-/-}$ islets is higher than in WT islets [11]. Since glucose-induced insulin secretion is lower in LDLR$^{-/-}$ islets, we investigated the relationship between cholesterol content, insulin secretion and $Ca^{2+}$ handling in these islets. Higher cholesterol content is associated with a decrease in fluidity [26] and an increase in the stiffness [27] of the membrane, and these alterations may cause an inappropriate distribution or functioning of membrane proteins. In this respect, alterations in the distribution and activity of ion channels and modifications of the distribution of SNARE proteins, linked to cholesterol clusters in the membrane, have been observed in pancreatic beta cells [28,29]. In addition, increased islet cholesterol levels caused by selective deletion of the *ABCA1* gene in apoE knockout mice result in reduced glucose-stimulated insulin secretion [30]. Furthermore, INS-1 cells overloaded with cholesterol secrete less insulin in response to glucose, possibly due to a reduction in glucokinase activity [8] that, ultimately, reflects alterations in membrane depolarization [31]. Here, we observed that glucose- and tolbutamide-induced insulin secretion as well as $Ca^{2+}$ handling in LDLR$^{-/-}$ islets was lower than in WT islets (Figs. 1 and 2). Moreover, SNAP-25 and VAMP-2 expression were reduced in LDLR$^{-/-}$ islets (Fig. 3). The lower expression of these two proteins, which participate in the trafficking of insulin-containing vesicles, could explain the lower insulin secretion observed during the second phase of insulin release in LDLR$^{-/-}$ islets. Cellular cholesterol also influences the trafficking of proteins from the cytosol to membrane raft microdomains [32] and is

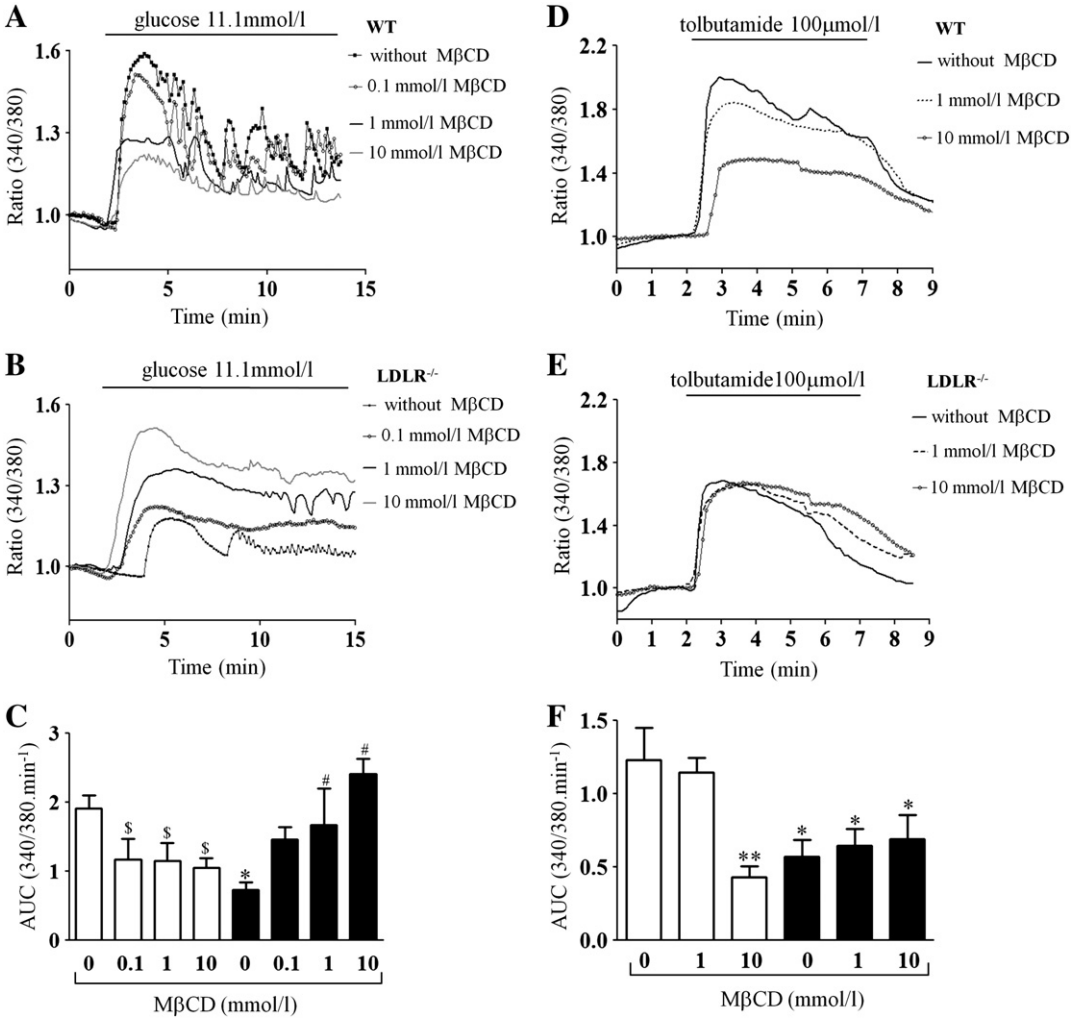


**Fig. 5.** Effects of MβCD treatment on the glucose- (A, B, C) or tolbutamide-induced (D, E, F) $[Ca^{2+}]_i$ rise in WT and LDLR$^{-/-}$ islets. (A) Representative curves of changes in intracellular $Ca^{2+}$ in response to 11.1 mmol/l glucose in WT and (B) LDLR$^{-/-}$ islets. (C) AUC of glucose-induced calcium rise in WT (open bars) and LDLR$^{-/-}$ islets (dark bars) treated with different concentrations of MβCD. (D) Representative curves of changes in intracellular $Ca^{2+}$ in response to 100 µmol/l tolbutamide in WT and (E) LDLR$^{-/-}$ islets. (F) AUC of tolbutamide-induced calcium rise in WT (open bars) and LDLR$^{-/-}$ islets (dark bars) in the presence of different concentrations of MβCD. Means ± SEM for 4–9 independent experiments. $^{*}p<0.05$ vs. WT (without MβCD) by *t*-test; $^{**}p<0.01$ vs. WT (without MβCD) by *t*-test; $^{\#}p<0.05$ vs. LDLR$^{-/-}$ (without MβCD) by one-way ANOVA; $^{\$}p<0.05$ vs. WT (without MβCD) by one-way ANOVA.

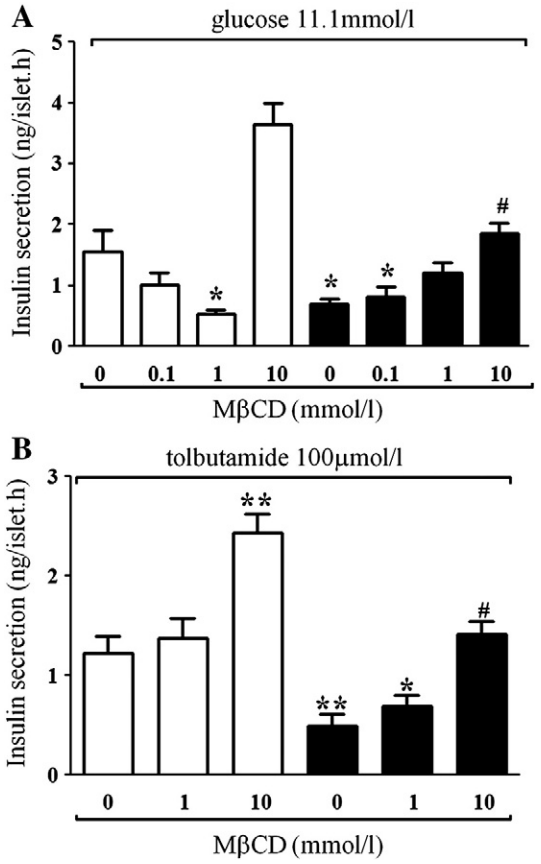


**Fig. 6.** Effects of cholesterol depletion on insulin secretion induced by 11.1 mmol/l glucose (A) or 100 μmol/l tolbutamide (B) in WT (open bars) and LDLR$^{-/-}$ islets (dark bars). Cholesterol depletion was promoted by pre-incubating the islets with 0.1, 1 or 10 mmol/l MβCD for 1 h at 37 °C. The bars represent the means ± SEM of 10–20 groups of islets from 8 different mice. $^{*}p<0.05$ vs. WT (without MβCD); $^{**}p<0.01$ vs. WT (without MβCD); $^{\#}p<0.05$ vs. LDLR$^{-/-}$ (without MβCD).

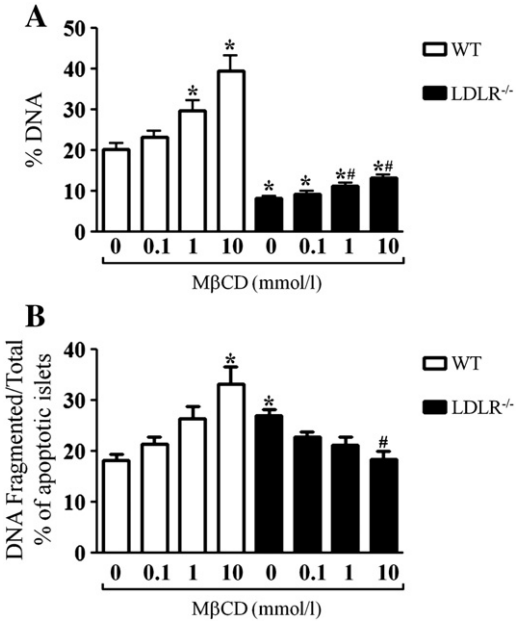


**Fig. 7.** Effects of cholesterol depletion on membrane integrity (A) and DNA fragmentation (B) in WT (open bars) and LDLR$^{-/-}$ islets (dark bars) pre-incubated with 0.1, 1 or 10 mmol/l MβCD for 1 h at 37 °C. Data are expressed as mean ± SEM of 8–12 independent experiments. $^{*}p<0.05$ vs. WT (without MβCD); $^{\#}p<0.05$ vs. LDLR$^{-/-}$.

important in coordinating the assembly of calcium channels with SNARE proteins during the exocytotic process [18,33]. Thus, the excess cholesterol observed in LDLR$^{-/-}$ islets may be responsible for the impairment of $Ca^{2+}$ handling and insulin secretion.

While high levels of cellular cholesterol impair glucose-induced insulin secretion, information concerning the reduction of cellular cholesterol is contradictory [8,16,18,31]. Here, we confirm that the removal of excess cholesterol from LDLR$^{-/-}$ islets by increasing concentrations of MβCD improved glucose-induced insulin secretion and that this improvement was linked to better $Ca^{2+}$ handling by these islets. Cholesterol-enriched mouse beta cells have a low voltage-gated calcium channel (VGCC) density, which diminishes $Ca^{2+}$ influx and, in turn, reduces insulin secretion [34]. Since, in the presence of MβCD, tolbutamide increased insulin secretion but did not modify the $Ca^{2+}$ signal in LDLR$^{-/-}$ islets, cholesterol normalization could improve some aspects of the $Ca^{2+}$-induced insulin release process other than VGCC density (not addressed in this study).

In contrast to the observations in LDLR$^{-/-}$ islets, when cholesterol was removed from WT islets treated with low concentrations of MβCD (0.1 and 1 mmol/l), the glucose-induced $[Ca^{2+}]_i$ rise was lower and insulin secretion was significantly reduced. However, at 10 mmol/l MβCD, a significant increase in insulin secretion was noticed, while $[Ca^{2+}]_i$ was lower than in WT without MβCD. Furthermore, in WT islets, the tolbutamide-induced $Ca^{2+}$ signal was also lowered by 10 mmol/l MβCD, whereas insulin secretion was increased. The reduction of cholesterol in rodent islets with a squalene epoxidase inhibitor (NB598) reduces insulin secretion, whole-cell delayed $Ca^{2+}$ currents, and granule mobilization. In MIN6 cells, NB598 also provokes a redistribution of membrane proteins, such as Kv2.1, Cav1.2, syntaxin-1A, SNAP-25, and VAMP [18]. We hypothesize that in the presence of lower concentrations of MβCD, several of the above-mentioned alterations obtained with NB598 may have occurred in our experiments, explaining the lower $Ca^{2+}$ handling and insulin secretion. However, the marked increase in insulin secretion induced by glucose or tolbutamide with low $Ca^{2+}$, in the presence of 10 mmol/l MβCD, has another explanation. In this case, the excessive removal of cholesterol from the membrane led to pore formation and the loss of membrane integrity, provoking a non-specific leakage of cytoplasmic content (Fig. 7A), including insulin release by a $Ca^{2+}$-independent mechanism. These changes in membrane integrity were, as expected, accompanied by an increase in apoptosis, as evidenced by the increased DNA fragmentation (Fig. 7B). It is also important to note that the administration of MβCD had the opposite effect on islets from LDLR$^{-/-}$ mice: lower apoptosis and DNA fragmentation (Fig. 7B). Thus, it is clear that the plasma membrane cholesterol content must be kept in an optimal range for optimal pancreatic islet function and survival.

In conclusion, glucose-induced insulin secretion and $Ca^{2+}$ handling were impaired in LDLR$^{-/-}$ compared with WT islets. In addition, SNAP-25 and VAMP-2, but not syntaxin-1A, were reduced in LDLR$^{-/-}$ islets. An adequate reduction of excess cholesterol normalized insulin secretion and $Ca^{2+}$ handling. However, a decrease in cholesterol in WT islets impaired $Ca^{2+}$ handling and insulin secretion. These data indicate that both excess and deficient cholesterol concentrations in islets alter glucose-induced $Ca^{2+}$ oscillations and, consequently, insulin secretion.

Supplementary data to this article can be found online at http://dx.doi.org/10.1016/j.bbalip.2012.12.013.

## Author contributions

Souza, JC: conception and experimental design, execution of all experiments, data interpretation, and manuscript writing; Vanzela EC: experimental execution and intellectual contribution; Ribeiro, RA and de Oliveira, CA: execution of insulin secretion and calcium experiments; Rezende, LF: experimental execution and intellectual

contribution; Carneiro, EM: intellectual contribution; Oliveira HCF and Boschero AC: conception and experimental design, data interpretation and reviewing the final version of the paper.

## Duality of interest

The authors declare that there is no duality of interest associated with this manuscript.

## Acknowledgements

This study was supported by these Brazilian foundations: Fundação de Amparo à Pesquisa do Estado de São Paulo (Fapesp), Coordenação de Aperfeiçoamento de Pessoal de Nível Superior (Capes), Conselho Nacional de Pesquisa (CNPq) and Instituto Nacional de Ciência e Tecnologia de Obesidade e Diabetes. We thank Mr. L. Domingos for the technical assistance. English was edited by the American Journal Experts (certificate AF57-9E6C-3B2D-33C4-C3B5).

## References

[1] M.J. Perley, D.M. Kipnis, Plasma insulin responses to oral and intravenous glucose: studies in normal and diabetic subjects, J. Clin. Invest. 46 (1967) 1954–1962.
[2] H.N. Ginsberg, Diabetic dyslipidemia: basic mechanisms underlying the common hypertriglyceridemia and low HDL cholesterol levels, Diabetes 45 (Suppl. 3) (1996) S27–S30.
[3] P.W. Wilson, D.L. McGee, W.B. Kannel, Obesity, very low density lipoproteins, and glucose intolerance over fourteen years: the Framingham Study, Am. J. Epidemiol. 114 (1981) 697–704.
[4] G.F. Lewis, A. Carpentier, K. Adeli, A. Giacca, Disordered fat storage and mobilization in the pathogenesis of insulin resistance and type 2 diabetes, Endocr. Rev. 23 (2002) 201–229.
[5] G.M. Reaven, Y.D. Chen, J. Jeppesen, P. Maheux, R.M. Krauss, Insulin resistance and hyperinsulinemia in individuals with small, dense low density lipoprotein particles, J. Clin. Invest. 92 (1993) 141–146.
[6] M.E. Cerf, High fat diet modulation of glucose sensing in the beta-cell, Med. Sci. Monit. 13 (2007) RA12–RA17.
[7] K. Eto, T. Yamashita, J. Matsui, Y. Terauchi, M. Noda, T. Kadowaki, Genetic manipulations of fatty acid metabolism in beta-cells are associated with dysregulated insulin secretion, Diabetes 51 (Suppl. 3) (2002) S414–S420.
[8] M. Hao, W.S. Head, S.C. Gunawardana, A.H. Hasty, D.W. Piston, Direct effect of cholesterol on insulin secretion: a novel mechanism for pancreatic beta-cell dysfunction, Diabetes 56 (2007) 2328–2338.
[9] L.R. Brunham, J.K. Kruit, T.D. Pape, J.M. Timmins, A.Q. Reuwer, Z. Vasanji, B.J. Marsh, B. Rodrigues, J.D. Johnson, J.S. Parks, C.B. Verchere, M.R. Hayden, Beta-cell ABCA1 influences insulin secretion, glucose homeostasis and response to thiazolidinedione treatment, Nat. Med. 13 (2007) 340–347.
[10] M. Ishikawa, Y. Iwasaki, S. Yatoh, T. Kato, S. Kumadaki, N. Inoue, T. Yamamoto, T. Matsuzaka, Y. Nakagawa, N. Yahagi, K. Kobayashi, A. Takahashi, N. Yamada, H. Shimano, Cholesterol accumulation and diabetes in pancreatic beta-cell-specific SREBP-2 transgenic mice: a new model for lipotoxicity, J. Lipid Res. 49 (2008) 2524–2534.
[11] M.L. Bonfleur, E.C. Vanzela, R.A. Ribeiro, G. de Gabriel Dorighello, C.P. de França Carvalho, C.B. Collares-Buzato, E.M. Carneiro, A.C. Boschero, H.C. de Oliveira, Primary hypercholesterolaemia impairs glucose homeostasis and insulin secretion in low-density lipoprotein receptor knockout mice independently of high-fat diet and obesity, Biochim. Biophys. Acta 1801 (2010) 183–190.
[12] J.C. de Souza, C.A. de Oliveira, E.M. Carneiro, A.C. Boschero, H.C. de Oliveira, Cholesterol toxicity in pancreatic islets from LDL receptor-deficient mice, Diabetologia 53 (2010) 2461–2462, (author reply 2463–2464).
[13] H. Ohvo-Rekilä, B. Ramstedt, P. Leppimäki, J.P. Slotte, Cholesterol interactions with phospholipids in membranes, Prog. Lipid Res. 41 (2002) 66–97.
[14] T. Róg, M. Pasenkiewicz-Gierula, Effects of epicholesterol on the phosphatidylcholine bilayer: a molecular simulation study, Biophys. J. 84 (2003) 1818–1826.
[15] O. Wiser, M. Trus, A. Hernández, E. Renström, S. Barg, P. Rorsman, D. Atlas, The voltage sensitive Lc-type Ca2 + channel is functionally coupled to the exocytotic machinery, Proc. Natl. Acad. Sci. U. S. A. 96 (1999) 248–253.
[16] F. Xia, X. Gao, E. Kwan, P.P. Lam, L. Chan, K. Sy, L. Sheu, M.B. Wheeler, H.Y. Gaisano, R.G. Tsushima, Disruption of pancreatic beta-cell lipid rafts modifies Kv2.1 channel gating and insulin exocytosis, J. Biol. Chem. 279 (2004) 24685–24691.
[17] J. Vikman, J. Jimenez-Feltström, P. Nyman, J. Thelin, L. Eliasson, Insulin secretion is highly sensitive to desorption of plasma membrane cholesterol, FASEB J. 23 (2009) 58–67.
[18] F. Xia, L. Xie, A. Mihic, X. Gao, Y. Chen, H.Y. Gaisano, R.G. Tsushima, Inhibition of cholesterol biosynthesis impairs insulin secretion and voltage-gated calcium channel function in pancreatic beta-cells, Endocrinology 149 (2008) 5136–5145.
[19] M.A. Rizzo, M.A. Magnuson, P.F. Drain, D.W. Piston, A functional link between glucokinase binding to insulin granules and conformational alterations in response to glucose and insulin, J. Biol. Chem. 277 (2002) 34168–34175.
[20] M.L. Bonfleur, R.A. Ribeiro, S.L. Balbo, E.C. Vanzela, E.M. Carneiro, H.C. de Oliveira, A.C. Boschero, Lower expression of PKAα impairs insulin secretion in islets isolated from low-density lipoprotein receptor (LDLR(−/−)) knockout mice, Metabolism 60 (2011) 1158–1164.
[21] A.C. Boschero, E. Delattre, The mechanism of gentamicin-inhibited insulin release by isolated islets, Arch. Int. Pharmacodyn. Ther. 273 (1985) 167–176.
[22] A.M. Scott, I. Atwater, E. Rojas, A method for the simultaneous measurement of insulin release and B cell membrane potential in single mouse islets of Langerhans, Diabetologia 21 (1981) 470–475.
[23] M.M. Bradford, A rapid and sensitive method for the quantitation of microgram quantities of protein utilizing the principle of protein-dye binding, Anal. Biochem. 72 (1976) 248–254.
[24] L.F. Rezende, A.S. Vieira, A. Negro, F. Langone, A.C. Boschero, Ciliary neurotrophic factor (CNTF) signals through STAT3-SOCS3 pathway and protects rat pancreatic islets from cytokine-induced apoptosis, Cytokine 46 (2009) 65–71.
[25] M.P. Czubryt, B. Ramjiawan, G.N. Pierce, The nuclear membrane integrity assay, Mol. Cell. Biochem. 172 (1997) 97–102.
[26] A. Colell, C. García-Ruiz, J.M. Lluis, O. Coll, M. Mari, J.C. Fernández-Checa, Cholesterol impairs the adenine nucleotide translocator-mediated mitochondrial permeability transition through altered membrane fluidity, J. Biol. Chem. 278 (2003) 33928–33935.
[27] J.A. Lundbaek, P. Birn, J. Girshman, A.J. Hansen, O.S. Andersen, Membrane stiffness and channel function, Biochemistry 35 (1996) 3825–3830.
[28] M.A. Churchward, T. Rogasevskaia, J. Höfgen, J. Bau, J.R. Coorssen, Cholesterol facilitates the native mechanism of Ca2 +-triggered membrane fusion, J. Cell Sci. 118 (2005) 4833–4848.
[29] N. Takahashi, H. Hatakeyama, H. Okado, A. Miwa, T. Kishimoto, T. Kojima, T. Abe, H. Kasai, Sequential exocytosis of insulin granules is associated with redistribution of SNAP25, J. Cell Biol. 165 (2004) 255–262.
[30] J.K. Kruit, P.H. Kremer, L. Dai, R. Tang, P. Ruddle, W. de Haan, L.R. Brunham, C.B. Verchere, M.R. Hayden, Cholesterol efflux via ATP-binding cassette transporter A1 (ABCA1) and cholesterol uptake via the LDL receptor influences cholesterol-induced impairment of beta cell function in mice, Diabetologia 53 (2010) 1110–1119.
[31] M. Hao, J.S. Bogan, Cholesterol regulates glucose-stimulated insulin secretion through phosphatidylinositol 4,5-bisphosphate, J. Biol. Chem. 284 (2009) 29489–29498.
[32] T. Lang, D. Bruns, D. Wenzel, D. Riedel, P. Holroyd, C. Thiele, R. Jahn, SNAREs are concentrated in cholesterol-dependent clusters that define docking and fusion sites for exocytosis, EMBO J. 20 (2001) 2202–2213.
[33] M. Ohara-Imaizumi, C. Nishiwaki, Y. Nakamichi, T. Kikuta, S. Nagai, S. Nagamatsu, Correlation of syntaxin-1 and SNAP-25 clusters with docking and fusion of insulin granules analysed by total internal reflection fluorescence microscopy, Diabetologia 47 (2004) 2200–2207.
[34] A.K. Lee, V. Yeung-Yam-Wah, F.W. Tse, A. Tse, Cholesterol elevation impairs glucose-stimulated Ca(2 +) signaling in mouse pancreatic β-cells, Endocrinology 152 (2011) 3351–3361.